Performance Analysis of Block Diagonalization Linear Precoding Technique on Multi User MIMO-GFDM System using MMSE Detector

Endah Wulansari[1], Titiek Suryani[1], and Endroyono[1]
[1]Department of Electrical Engineering
Institut Teknologi Sepuluh Nopember, Surabaya Indonesia 60111
Email: endah.wulansari16@mhs.ee.its.ac.id, titiks@ee.its.ac.id, endroyono@ee.its.ac.id

***Abstract*— The implementation of the MIMO system for services to multiple users (known as Multi User-MIMO) is required for 5G communication systems. Generalized Frequency Division Multiplexing (GFDM) is a flexible multi-carrier transmission with non-orthogonal waveforms and fewer subcarriers are able to overcome OFDM weaknesses, namely high peak-to-average power ratio (PAPR) and out-of-band (OOB) emissions. The existence of MU-MIMO cause interference among users that can be overcome with Block Diagonalization linear precoding technique. The use of multiple antennas on each user can be mitigated by detector techniques. In this paper, we analyze the combined performance of BD precoding on the transmitter and the Minimum Mean Square Error (MMSE) detector on the receiver of the MU MIMO-GFDM system. The simulation results show that MU MIMO-GFDM using root raised cosine (RRC) pulse superior to MU MIMO-OFDM using rectangular pulse in BER and PAPR performance.**

***Keywords*— MU-MIMO, GFDM, Block Diagonalization (BD), Minimum Mean Square Error (MMSE), PAPR**

List of symbols

$\boldsymbol{u}$	: desired user	$\boldsymbol{k}$	: interfering user
$\boldsymbol{x}$	: GFDM signal	$\boldsymbol{y}$	: received signal
$\boldsymbol{n}$	: noise	$\boldsymbol{\sigma_n^2}$	: noise variance
$\boldsymbol{s}$	: transmitted signal	$\boldsymbol{\alpha}$	: roll of factor
$\boldsymbol{M}$	: subsymbol	$\boldsymbol{K}$	: subcarrier
$\boldsymbol{N}$	: GFDM block	$\boldsymbol{W}$	: precoding matrix
$\boldsymbol{H}$	: channel matrix	$\boldsymbol{d_{k,m}}$	: data block
$\boldsymbol{g_{k,m}}$	: prototype filter	$\boldsymbol{z}$	: threshold level
$\boldsymbol{P_{peak}}$	: peak power	$\boldsymbol{P_{average}}$	: average power

$\boldsymbol{N_T}$: transmitter antenna

$\boldsymbol{N_{R,k}}$: receiver antenna in each user

$\boldsymbol{N_{R,total}}$: antenna total of all users in receiver

$\boldsymbol{H_{eff,u}}$: effective MIMO channels

$\boldsymbol{W_{MMSE}}$: weight matrix of MMSE

I. INTRODUCTION

Multiple-Input Multiple-Output (MIMO) technique is considered to increase high data rates transmission and spectrum efficiency. Orthogonal Frequency Division Multiplexing (OFDM) technique as multicarrier modulation is used in MIMO to overcome multipath channel. Hence, joint of MIMO and OFDM techniques are the right choice [1,2,3]. To migrate from 4G technology to the next mobile technology, scenarios for 5G technology should be fulfilled. Such scenarios include increasing capacity system, high Quality of Service (QoS), low power consumption, and low latency [4]. GFDM is one of the waveform candidates which currently considered and evaluated by the 5GNow team [5]. GFDM is able to overcome the weakness of OFDM that is high PAPR and OOB radiation. GFDM produces a low PAPR because the number of subcarrier used less and resistance for non-linear distortion [6]. GFDM is able to produce low OOB emissions by using pulse shaping raised cosine and the use of a single CP on a set of GFDM symbol groups generate efficient bandwidth [7,8].

Nowaday advanced research is directed to the implementation of MIMO systems for services to many users (known as Multi User-MIMO). In the MU-MIMO system, a Base Station (BS) with multiple antennas emits signals to multiple users, which each user has more than one receiver antenna. A BS requires the application of orthogonal techniques to allocate each user on different spatial dimensions to get minimum interference [9,10]. The existence of interference generated by inter-antennas on each user, hence required detector technique on receiver. Known detector technique is Zero Forcing (ZF) and Minimum Mean-Square Error (MMSE) [11]. ZF could not remove the inter-antenna interference (IAI) perfectly due to noise enhancement. MMSE was selected to conquer ZF's weaknesses and maximize signal-to-interference plus noise ratio (SINR) values.

The channel capacity for MU-MIMO has been analyzed using a technique called "writing on dirty paper" [12]. If the transmitter carried out the early interference removal process through the precoding process in the transmitter, so that the receiver complexity can be significantly simplified. When the MU-MIMO is adopted, spatial multiplexing gain to increase the system capacity will be obtained [10].

The capacity value for the MU-MIMO downlink channel can be found through the application of Dirty Paper Coding

978-1-5386-2373-2/17/$31.00 ©2017 IEEE

(DPC) techniques [9,11,13]. Optimal precoding of MU-MIMO is based on the DPC theory which developed by Costa with non-linear precoding method. On the transmitter DPC has known the signal interferences, so the use of precoding on the transmitter side can eliminate the interference and reach the sum capacity of MU-MIMO downlink channel. However DPC is not suitable to be implemented in practical systems due to its high complexity [9,10]. To reduce the computational complexity in eliminating interference among users is used linear precoding technique. Linear precoding techniques are known as channel inversion (CI) and block diagonalization (BD) [9,11]. CI uses traditional MIMO detectors such as ZF and MMSE. Precoding performed on the transmitter in CI with ZF detector can be used to suppress CCI completely, but it raises noise enhancement because the precoding vector is not normalized. To solve them, it can be used CI with MMSE, but this system could not reach the best system performance because it is used for single antenna, so it could not be implemented for MU MIMO-GFDM system using multi antenna for each user [11].

To overcome the weaknesses of DPC and CI precoding, BD technique was developed. BD has a capable orthogonal scheme can achieve sum capacity and low complexity. BD decomposes a MU-MIMO downlink channel into multiple channel of single user-MIMO downlink in parallel. Each user signal multiplied by a precoding matrix before being transmitted by placing all other user channel matrices in null space. So the interferences from other users (called Multi User Interferences~MUI) are efficiently made zero. If the channel matrices of all users are fully recognized in the transmitter (known as Channel State Information~CSI), then each user has an interference-free channel from other users [9,11,14-16].

In the previous study [1-16], there was no discussion of the combined BD technique applied on the transmitter and MMSE applied on the receiver end of the MU-MIMO system on the 5G technology using GFDM waveform. The use of MU MIMO-GFDM can fullfill the demands of 5G wireless communications systems.The novel aspect of this research is the application of BD on the MU MIMO-GFDM system. While the superiority of this research is BD and MMSE combined scheme on MU MIMO-GFDM system able to overcome MUI and IAI with low complexity. The paper contribution structure will be shown as follows: Section II shows the system model, Section III discusses GFDM as 5G waveform, Section IV describes the BD algorithm, Section V discusses the calculation of PAPR, the simulation results are described in Section VI. Finally, Section VII concludes our work.

II. System Model

In this section the broadcast narrow-band signal and MU-MIMO channels are assumed to be flat fading using GFDM that work on a non-line-of-sight rich scattering environment. The system uses perfect CSI in transmitter. Fig. 1 illustrates the MU MIMO-GFDM system model using downlink channel scenario, where base station with multiple N_T antennas send a row of data to K user, each one or more $N_{R,k}$ receiver antennas.

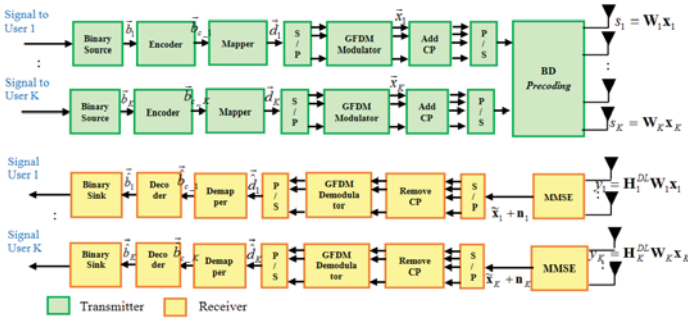

Fig. 1. MU MIMO-GFDM Transceiver System Model

A. MU MIMO-GFDM Transmitter

On the transmitter, a BS sends data to K-user. Rows of mapper result symbols processed through GFDM modulator will generate x_k using 16-Offset QAM which will be discussed in detail in section III. 16-OQAM modulation is used on MU MIMO-GFDM using RRC pulse. Since GFDM has a non-orthogonal waveform, then by using OQAM the orthogonality of a waveform can be obtained and the low OOB emission can be reached. The Output of GFDM modulator using 16-OQAM will be the BD precoding input as x_k which will be multiplied by the $\mathbf{W}_k$ precoding matrix and put it on the other user's channel matrix in null space. The signal transmitted through the transmitter shown in (1).

$$s_k = \sum_{k=0}^{K} \mathbf{W}_k \mathbf{x}_k \tag{1}$$

Signals are transmitted through multiple antennas using spatial multiplexing techniques, where each transmitter antenna sends a row of different data to increase the system capacity.

B. Channel Model

After passing through MU MIMO-GFDM transmitter then GFDM signal is obtained $x_{GFDM} = x[0], x[1], \cdots, x[N-1]$, where N is block GFDM. Because using MU MIMO-GFDM with BD, before GFDM signal $\vec{x}$ which use 16-OQAM transmitted will be multiplied by the precoding matrix ($\mathbf{W}$) as described in section IV to eliminate interference among users. Transmission through AWGN channel can be modeled by:

$$\vec{y} = \mathbf{H}\vec{s} + \vec{n} = \mathbf{HW}\vec{x} + \vec{n} \tag{2}$$

where $\vec{n} \sim \mathrm{CN}(0, \sigma_n^2 \mathbf{I}_{MN})$ is AWGN vector with noise variance σ_n^2 and $\mathbf{I}_{MN}$ is identity matrix $MN \times MN$, where M is subsymbol and N is GFDM block. $\mathbf{H}$ is channel matrix using convolution matrix with diagonal structure based on $\vec{h} = [h_0, .., h_{N_{CH}-1}]^T$ into impulse response channel of length N_{ch} [8].

After passing the wireless channel as in (2), the received signal is represented in (3):

$$\mathbf{y}_\mathrm{u} = \mathbf{H}_u^{\mathrm{DL}} \textstyle\sum_{k=1}^{K} s_k + \mathbf{n}_u$$

$$= \mathbf{H}_u^{\mathrm{DL}} \sum_{k=1}^{K} \mathbf{W}_k \mathbf{x}_k + \mathbf{n}_u$$

$$= \mathbf{H}_u^{\mathrm{DL}}\mathbf{W}_u\mathbf{x}_u + \sum_{\substack{k=1 \\ k\neq u}}^{K} \mathbf{H}_k^{\mathrm{DL}}\mathbf{W}_k\mathbf{x}_k + \mathbf{n}_u \quad (3)$$

where $\mathbf{y}_u \in \mathbb{C}^{N_{R,u}\times 1}$ is the signal that received by user, $\mathbf{x}_u \in \mathbb{C}^{N_{R,u}\times 1}$ is the uth user estimated signal, $\mathbf{H}_u^{\mathrm{DL}} \in \mathbb{C}^{N_{R,u}\times N_T}$ is a downlink channel matrix between BS and uth user assumed to be independent fading, $\mathbf{W}_u \in \mathbb{C}^{N_T\times N_{R,u}}$ is the uth user precoding matrix, K is the number of users, and $\mathbf{n}_u$ is noise vector of the uth user that represents the zero-mean AWGN vector with variance σ_n^2. Equation (3) can be shown in Fig. 2 which is the multi-user downlink MIMO using BD precoding [16].

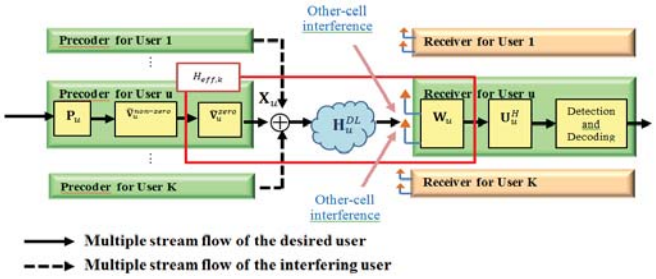

Fig. 2. Downlink MU-MIMO using BD Precoding

The signal received by K user as in (3) is represented in the following matrix, as in (4).

$$\begin{bmatrix} y_1 \\ y_2 \\ \vdots \\ y_K \end{bmatrix} = \begin{bmatrix} \mathrm{H}_1^{\mathrm{DL}}\mathrm{W}_1 & \mathrm{H}_1^{\mathrm{DL}}\mathrm{W}_2 & \cdots & \mathrm{H}_1^{\mathrm{DL}}\mathrm{W}_K \\ \mathrm{H}_2^{\mathrm{DL}}\mathrm{W}_1 & \mathrm{H}_2^{\mathrm{DL}}\mathrm{W}_2 & \cdots & \mathrm{H}_2^{\mathrm{DL}}\mathrm{W}_K \\ \vdots & \vdots & \ddots & \vdots \\ \mathrm{H}_K^{\mathrm{DL}}\mathrm{W}_1 & \mathrm{H}_K^{\mathrm{DL}}\mathrm{W}_2 & \cdots & \mathrm{H}_K^{\mathrm{DL}}\mathrm{W}_K \end{bmatrix} \begin{bmatrix} \tilde{\mathrm{x}}_1 \\ \tilde{\mathrm{x}}_2 \\ \vdots \\ \tilde{\mathrm{x}}_K \end{bmatrix} + \begin{bmatrix} \mathrm{n}_1 \\ n_2 \\ \vdots \\ \mathrm{n}_K \end{bmatrix} \quad (4)$$

To eliminate interference among users in MU MIMO-GFDM system will be used BD precoding using Singular Value Decomposition (SVD) as described in Section IV.

C. MU MIMO-GFDM Receiver

In MIMO system with multiple antennas at the receiver, each antenna will receive many signals from the transmitter. The received signal will being distorted by fading, channel noise, and IAI which can degrade the system performance. For IAI mitigation, each receiver must add MIMO detector one of which is MMSE.

To get $\tilde{\mathrm{x}}_\mathrm{u}$ in the MMSE detector is to determine the weight of $\mathbf{W}_{\mathrm{MMSE}}$ as in (5). $\mathbf{H}$ is assumed the ideal channel estimation is known completely or perfect CSI in the transmitter.

$$\mathbf{W}_{MMSE} = \left(\mathbf{H}^{\mathrm{H}}\mathbf{H} + \frac{1}{SNR}\mathbf{I}\right)^{-1}\mathbf{H}^{\mathrm{H}} \quad (5)$$

With the application of BD precoding to detect interference from other user, the channel matrix becomes $\mathbf{H}_u\mathbf{W}_u = \mathbf{H}_u^{\mathrm{DL}}\mathbf{W}_u$. After the channel is multiplied, the equation $\mathbf{W}_{\mathrm{MMSE}}$ becomes:

$$\mathbf{W}_{MMSE} = \left((\mathbf{H}_u^{\mathrm{DL}}\mathbf{W}_u)^{\mathrm{H}}(\mathbf{H}_u^{\mathrm{DL}}\mathbf{W}_u) + \frac{1}{SNR}\mathbf{I}\right)^{-1}(\mathbf{H}_u^{\mathrm{DL}}\mathbf{W}_u)^{\mathrm{H}} \quad (6)$$

Thus, the estimated value of $\tilde{\mathrm{x}}_\mathrm{u}$ can be obtained:

$$\tilde{\mathbf{x}}_u = \mathbf{W}_{MMSE}\mathbf{y}_u \quad (7)$$

III. GFDM Waveform

A. GFDM Modulator

GFDM is 5G waveform that adopts the principle of OFDM. GFDM is multi-carrier modulation scheme that related to flexible pulse shaping and based on independent block modulation. The difference in frequency and time partition between OFDM and GFDM [8] which can be influence on the system work. The OFDM signal is the sum of several N subcarriers with $1/T$ intervals carrying several symbols that have been distinguished its timeslot. While the GFDM signal is a sum of separate $K\,subcarrier \times M\,subsymbol$ sized blocks with M/T intervals distributed to all M timeslot and K-frequency slots, where T is time period.

According to Fig.1, $\vec{b}$ binary input generated by the binary source is encoded into $\vec{b}_c$. The encoding result will be mapped into mapper block. The output of mapper is data block $\vec{d}$ is converted to low data rate and decomposed into GFDM blocks. Each subsymbol of the decomposition will be up-sampling with a N factor which aims to convert impulse signals. $d_{k,m}$ data block is an individual elements correspond to the data transmitted on $k-th$ subcarrier and $m-th$ subsymbol of N block. $d_{k,m}$ is bounded by nature independent and identically distributed i.i.d. with variance and taken from the mapper signal output. Furthermore the output of each up-sampling blocks will be circularly constructed with a prototype filter $g_{k,m}[n]$ and shifted by K/N at frequency with $1/N$ subcarrier intervals, as in (8) [8].

$$g_{k,m}[n] = g[(n-mK)mod\ N]e^{-j2\pi\frac{k}{K}n} \quad (8)$$

Equation (8) consists of two components are $[(n-mK)mod\ N]$ which work to shift at time domain as a differentiator between subsymbol based on timeslot and complex exponential numbers $e^{-j2\pi(k/K)n}$ work to shift at frequency domain.

MU MIMO-GFDM system using RRC pulse and OQAM modulation. In GFDM-OQAM, orthogonality of a waveform can be obtained and low OOB can be reached by transmitting $d_{k,m}^{(i)}$ and $d_{k,m}^{(q)}$ respectively are the real and imaginary parts of $d_{k,m}$ using real-valued, half prototype filter $g_{k,m}[n]$ with offset of $M/2$ samples and phase rotation of $\pi/2$ radians among adjacent subsymbol and subcarrier. Mathematically, the GFDM signals using O-QAM is given by [17]:

$$x[n] = \sum_{k=0}^{K-1}\sum_{m=0}^{M-1} d_{k,m}^{(i)}\, g_{k,m}^{(i)}[n] + \sum_{k=0}^{K-1}\sum_{m=0}^{M-1} d_{k,m}^{(q)}\, g_{k,m}^{(q)}[n] \quad (9)$$

The GFDM signal transmitted in (9) can be rewritten as in (10). Based on (9) and (10), the column of matrix $\mathbf{A}^{(i)}$ and $\mathbf{A}^{(q)}$ carry $g_{k,m}^{(i)}$ and $g_{k,m}^{(q)}$ respectively [17].

$$x = \mathbf{A}^{(i)}\mathbf{d}^{(i)} + \mathbf{A}^{(q)}\mathbf{d}^{(q)} \quad (10)$$

Equation (10) can be rewritten as in (11)

$$\vec{x} = \mathbf{A}\vec{d} \quad (11)$$

$\vec{x}$ is a column vector consisting of an $x[n]$ GFDM signal. The transmitter matrix has size $KM \times KM$ with complex data

symbols $\vec{d}$ and **A** consists of data symbols shifted by prototype filter $g_{k,m}$ as in (8) [8].

Before transmitted in wireless channel, GFDM signal added CP to mitigate intersymbol interference among GFDM blocks. The use of one CP on each GFDM block, thus GFDM could enhance the efficiency bandwidth while compared to OFDM.

B. Pulse Shaping Filter

One of method for ISI mitigation is shaping the transmitted signals. In GFDM, pulse shaping used is RRC developed from raised cosine (RC). Pulse shaping is designed at time domain based on a roll of factor α as in (12) [19]. Range of roll of factor is $0 < \alpha < 1$.

$$g_{RC}(t) = \begin{cases} 1, & for\ |t| \le (1-\alpha)\frac{T}{2} \\ \frac{1}{2}\left[1 + cos\left(\pi\left(\frac{|t| - (1-\alpha)\frac{T}{2}}{\alpha T}\right)\right)\right], & for\ (1-\alpha)\frac{T}{2} < |t| \le (1+\alpha)\frac{T}{2} \\ 0, & others \end{cases} \quad (12)$$

To obtain the half-Nyquist RRC pulse ($g(t)$) is taking the square root of $g_{RC}(t)$. The Meyer RRC pulse proposed in this thesis combines the RRC pulse with the Meyer auxiliary function at time domain [19], as follows:

$$g(t) = \sqrt{g_{RC}(t)} \quad (13)$$

where the Meyer auxilary function [19] is:

$$w(t) = t^4(35 - 84t + 70t^2 - 20t^3) \quad (14)$$

C. GFDM Demodulator

The process in the receiver after signal detection as described in section II is the CP removal then followed by the GFDM demodulator. Furthermore the output of GFDM demodulator are processed by demapper to generate a sequence of symbol in the receiver is $\hat{b}_c$. Then decoding done to change $\hat{b}_c$ become $\hat{b}$.

IV. Block Diagonalization Algorithm In MU MIMO-GFDM Transmission Model

BD processing in the transmitter to eliminate multi-user interference (MUI) by using precoding matrix $\mathbf{W}_k$. The transmitter assumed knows perfect Channel State Information.

BD implementation scheme on MU MIMO-GFDM transmission system for K-users as in Fig. 3 with size of channel matrix $\mathbf{H}_u^{\mathrm{DL}} \in \mathbb{C}^{\mathrm{N_{R,total}} \times N_T}$, which $\mathrm{N_{R,total}} = \sum_{u=1}^{K} N_{R,u} = N_T$. $\mathrm{N_{R,total}}$ is antenna total of all users in the receiver, $N_{R,u}$ is the number of antennas each user, and N_T is the number of antennas in the base station [11].

Multiplication results $\mathbf{H}_k\mathbf{W}_k$ into block diagonal due to the size of matrix $\mathrm{N_{R,total}} = N_T$, thus the algorithm is called Block Diagonalization where $\mathbf{H}_k = [\mathbf{H}_1^T \quad \mathbf{H}_2^T \quad \cdots \quad \mathbf{H}_K^T]^T$ and $\mathbf{W}_k = [\mathbf{W}_1 \quad \mathbf{W}_2 \quad \cdots \quad \mathbf{W}_K]$ [15].

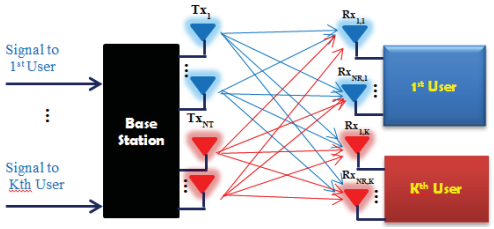

Fig. 3. MU MIMO-GFDM Transmission Scheme with BD Precoding

The known CSI in transmitter cause the transmitter could recognize its signals interference, So the matrix $\sum_{k=1,k\neq u}^{K} \mathbf{H}_u^{DL}\mathbf{W_k}\tilde{\boldsymbol{x}}_{\boldsymbol{k}}$ in (3) causes interference to u^{th} user should be eliminated, hence $\{\mathbf{H}_u^{DL}\mathbf{W_k}\}_{u\neq k}$ will be as zero matrix as in (15).

$$\mathbf{H}_u^{\mathrm{DL}}\mathbf{W}_k = \mathbf{0}_{N_{\mathrm{R},u}\times N_{\mathrm{R},u}},\ \forall\, u \neq k \quad (15)$$

To resolve the constraint of total transmit power, $\mathbf{W}_u \in C^{N_T \times \mathrm{N_{R,u}}}$ precoding must be unitary, thus the signal matrix of all free MUI users in (4) is expressed as in (16).

$$\begin{bmatrix} y_1 \\ y_2 \\ \vdots \\ y_K \end{bmatrix} = \begin{bmatrix} \mathrm{H_1^{DL}W_1} & 0 & \cdots & 0 \\ 0 & \mathrm{H_2^{DL}W_2} & \cdots & 0 \\ \vdots & \vdots & \ddots & \vdots \\ 0 & 0 & \cdots & \mathrm{H_K^{DL}W_K} \end{bmatrix} \begin{bmatrix} \mathrm{x_1} \\ \mathrm{x_2} \\ \vdots \\ \mathrm{x_K} \end{bmatrix} + \begin{bmatrix} \mathrm{n_1} \\ \mathrm{n_2} \\ \vdots \\ \mathrm{n_K} \end{bmatrix} \quad (16)$$

To estimate $\tilde{x}_u$ used MMSE signal detection as described in section II. In order the $\{\mathbf{W}_k\}_{k=1}^{K}$ matrix is fulfilled in equation (15), channels matrix are made consists of the all user channel gain except the u^{th} user, as in (17).

$$\tilde{\mathbf{H}}_u^{DL} = [(\mathbf{H}_1^{DL})^H \quad \cdots \quad (\mathbf{H}_{u-1}^{DL})^H \quad (\mathbf{H}_{u+1}^{DL})^H \quad \cdots \quad (\mathbf{H}_K^{DL})^H]^H \quad (17)$$

$\mathbf{W}_u \in C^{N_T \times \mathrm{N_{R,u}}}$ precoding matrix should be designed as null space of $\tilde{\mathbf{H}}_u^{DL}$. SVD is based on the algebra linear theorem and is said to rectangular matrix **H** by diagonalizing a matrix and obtaining its eigenvalue. It aims to estimate the channel response matrix. By applying SVD, the orthogonal basis of channel matrix $\tilde{\mathbf{H}}_u^{DL}$ can be decomposed as in (18) [11].

$$\tilde{\mathbf{H}}_u^{DL} = \tilde{\mathbf{U}}_u\tilde{\mathbf{\Omega}}_u[\tilde{\mathbf{V}}_u^{non-zero} \quad \tilde{\mathbf{V}}_u^{zero}]^H \quad (18)$$

where the column of **U** are orthonormal eigenvectors of $\mathbf{HH^T}$, the column of **V** are orthonormal eigenvectors of $\mathbf{H^TH}$, and **Ω** is a diagonal matrix containing the square roots of eigenvalues from **U** and **V** in descending order. In equation (18), $\tilde{\mathbf{V}}_u^{non-zero} \in C^{\left(\mathrm{N_{R,total}} - N_{R,u}\right)\times N_T}$ and $\tilde{\mathbf{V}}_u^{zero} \in C^{N_{R,u}\times N_T}$ are arranged in the right singular vector based on non-zero singular value and zero singular value. The multiplication of $\tilde{\mathbf{H}}_u^{DL}$ and $\tilde{\mathbf{V}}_u^{zero}$ made zero.

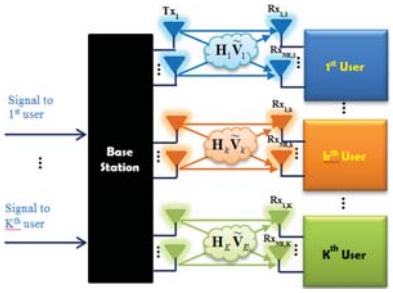

Fig. 4. Channels Condition of Null Space After Precoding Matrices Addition

From the multiplication channel matrix and precoding, $\widetilde{\mathbf{V}}_u^{zero}$ is the null space of $\widetilde{\mathbf{H}}_u^{DL}$, so the signal transmitted on the $\widetilde{\mathbf{V}}_u^{zero}$ by placing another user signal is zero. Then $\mathbf{W}_u = \widetilde{\mathbf{V}}_u$ is used as u^{th} user's precoding. By precoding $\{\mathbf{W}_k\}_{k=1}^{K}$, MUI is perfectly eliminated and SU-MIMO downlink channels are formed in parallel between user and BS as shown in Fig. 4. Thus, the effective MIMO channels for u^{th} user are described [9,11] as in (19).

$$\mathbf{H}_{eff,u} = \mathbf{H}_u \widetilde{\mathbf{V}}_u^{zero} \tag{19}$$

V. Peak To Average Power Ratio (PAPR)

PAPR is the ratio of peak signal power to average power. PAPR occurs due to the multi-carrier system consists of an independently modulated subcarrier summation. If each phase of subcarrier is equal then it would generate peak signal power equal to N times its average power. Peak power is the power of sinusoidal wave with amplitude equal to maximum envelope [11,18]. PAPR is shown mathematically in (20).

$$PAPR = \frac{P_{peak}}{P_{average}} = 10\, log_{10} \frac{max|s(t)|^2}{E\{|s(t)|^2\}} \tag{20}$$

where P_{peak} is peak power, $P_{average}$ is average power, $s(t)$ is multi-carrier signal of continuous time and $E[.]$ is expectation.

PAPR values are statistically described using the Complementary Cumulative Distribution Function (CCDF). CCDF is a parameter used to measure peak power from signal containing information about PAPR above a certain level. When the IFFT input signal with N subcarrier is independent and the magnitude distributed uniform, it is assumed that the real and imaginary part of a Gaussian distributed $s(t)$ signal with an average value of 0 and a variance of 0.5. Assumed average signal power $E\{|s(t)|^2\} = 1$. So PAPR CCDF value of the data block is mathematically formulated as follows with z is a threshold level.

$$\begin{aligned} P(PAPR > z) &= 1 - P(PAPR \leq z) \\ &= 1 - [1 - \exp(-z)]^N \end{aligned} \tag{21}$$

VI. Experiment And Simulation Result

In this section, to find out the performance of combination BD technique applied on the transmitter and MMSE applied on the receiver end of the MU-MIMO system on the 5G technology using GFDM waveform, we compare the performance of BER, PAPR, and OOB of MU MIMO-GFDM systems and MU MIMO-OFDM systems for comparative analysis. Assumed the system uses perfect CSI in transmitter and the channel condition is ideal.

A. Bit Error Rate (BER) Analysis

Simulation of system performance comparison is shown by parameter as in table 1. Fig. 5. shows the performance of MU MIMO-GFDM and MU MIMO-OFDM on MIMO 2x2 with 4 users on AWGN channel and the channel matrices of all users are fully recognized in the transmitter (perfect CSI).

In our work simulated MU MIMO-GFDM using pulse shaping RRC (α = 1 ; 16-OQAM) and MU MIMO-GFDM using rectangular pulse (α = 0 ; 16QAM). MU MIMO-GFDM with two different waveforms compared with MU MIMO-OFDM using rectangular pulse (α = 0 ; 16-QAM).

TABLE I. Simulation Parameter

Parameter	Notation	Type and Parameter Value	
		MU MIMO-OFDM	MU MIMO-GFDM
Modulation	-	16-QAM	16-QAM ; 16-OQAM
Transmit-receive antenna scheme	N_t x $N_{R,u}$	2x2	2x2
Number of bits sent	N_bit	1024000 bit	1024000 bit
Number of packets	N_packet	5	5
Number of users	N_user	2 and 4	2 and 4
Channel	-	AWGN	AWGN
Signal Detection	-	MMSE	MMSE
Pulse shaping	-	*Rectangular*	*Rectangular;* RRC
Roll of factor	α	0	0 and 1
Number of subcarrier	Nc	310	310
Number of sample per symbol	Nfft	512	512
Subcarrier	K	310	10
Subsymbol	M	1	31

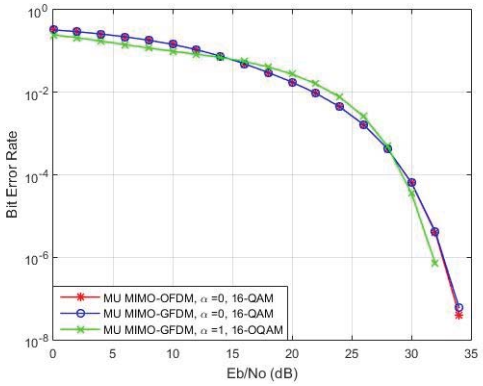

Fig. 5. System Performance Comparison of MU MIMO-GFDM and MU MIMO-OFDM On MIMO 2x2

In 16-QAM modulation, 4 bits are mapped into one symbol. These 16 combinations are divided into 4 combinations for each real and imaginary quadrant. On one of quadrant for positive real and positive imaginary, then 4 bit combinations are mapped into 4 symbols i.e $1+j, 1+3j, 3+j, 3+3j$. Each symbol needs $(1^2+1^2+1^2+3^2+3^2+1^2+3^2+3^2)/4 = 10$ power which if converted to voltage being $\sqrt{10}$. To generate $E\{|s(t)|^2\} = 1$, signals are multiplied by $1/\sqrt{10}$. Another way can be calculated $\sqrt{3/2(M-1)} = \sqrt{3/2(16-1)} = 1/\sqrt{10}$, with M is the modulation index. 16-OQAM modulation is bits in the inphase position remain at initial position while offset occurs or bit shifting on quadrature side of $M/2$.

Based on the Fig. 5, the performance of MU MIMO-OFDM and MU MIMO-GFDM systems using rectangular pulse produces the same performance. This is due to the parameters used are same, the difference only in how to bring information data to data transmitting from the transmitter to receiver. In MU MIMO-GFDM uses block systems which consists of

K subcarrier and M subsymbol. While on MU MIMO-OFDM only use K subcarrier consisting of subcarrier and subsymbol multiplication on MU MIMO-GFDM.

The performance of MU MIMO-GFDM using pulse shaping RRC (α = 1;16-OQAM) resulted better performance ± 0.84dB than MU MIMO-OFDM and MU MIMO-GFDM using rectangular pulse (α = 0;16QAM). This is because MU MIMO-GFDM with RRC to achieve orthogonality at the transmitted signal and to reach low OOB that should do the Offset QAM modulation, so MU MIMO-GFDM with RRC should use O-QAM modulation to achieve good performance and to resolve non-orthogonal conditions on GFDM. In addition, the MU MIMO-OFDM and MU MIMO-GFDM systems use the ideal channel estimation of the AWGN channel where noise as interferer, so both of the systems have the same performance. They successfully eliminate MUI using BD precoding and eliminate IAI using MMSE detectors.

B. Peak to Average Power Ratio (PAPR) Analysis

Simulation is shown with parameter as in table 1. On MU MIMO-GFDM uses block systems consisting of $K = 10$ subcarriers and $M = 31$ subsymbols, while MU MIMO-OFDM consists of $K \times M = 310$ subcarriers. In this study, we investigate the effect of waveform subcarrier number that result a different PAPR. Comparison of PAPR between MU MIMO-GFDM which use rectangular and RRC pulse and MU MIMO-OFDM which use rectangular pulse using Nfft = 512, MIMO 2x2 and two users are shown in Fig. 6. PAPR curve in Fig.6 can be obtained by using formula as in (20). CCDF plotting with the x-axis is the PAPR (dB) and the y-axis is the probability $P_r(PAPR_s \leq PAPR)$.

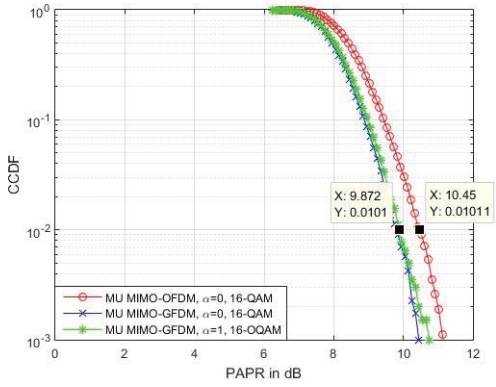

Fig. 6. Comparison CCDF of PAPR for System Performance

Based on Fig. 6, in the observation of CCDF=10^{-2}, the PAPR value of MU MIMO-GFDM with different pulse shaping (RRC pulse and rectangular pulse) is better ± 0.578dB than MU MIMO-OFDM with rectangular pulse. From the result, the PAPR value of MU MIMO-GFDM is lower than MU MIMO-OFDM. This is due to the peak value of OFDM or GFDM signal is N times from the peak of each subcarrier. So larger the number of subcarrier hence the PAPR value becomes high. Since MU MIMO-GFDM in frequency and time partition using block systems where each block consists of subcarrier and subsymbol multiplication and MU MIMO-OFDM only use K subcarrier consisting of subcarrier and subsymbol multiplication on MU MIMO-GFDM, so the use of MU MIMO-GFDM subcarriers is less than MU MIMO-OFDM.

C. Out-of-Band (OOB) Analysis

The OOB radiation simulation is shown by the parameter as in Table 1, where MU MIMO-GFDM system using RRC pulse (α = 1; 16-OQAM) and rectangular pulse (α = 0; 16-QAM), while MU MIMO-OFDM system using rectangular pulse (α = 0; 16-QAM). The observation of OBB radiation can be seen from shaping the transmission signal.

To observe OOB radiation in MU MIMO system using both OFDM and GFDM waveform can be seen from the power spectral density (PSD) function of frequency (f). To observe the OOB (PSD) of a waveform, which processes the output signal waveform (OFDM or GFDM) of the FFT process, and then proceeds with the PSD calculation of a waveform. The PSD calculation of simulation uses the "pwelch" function, i.e. searching for DFT (based on FFT algorithm), then squaring the magnitude value. Fig. 7 shows the OOB curve between the MU MIMO-GFDM using rectangular pulse and RRC pulse, and MU MIMO-OFDM using rectangular pulse on MIMO 2x2 with two users.

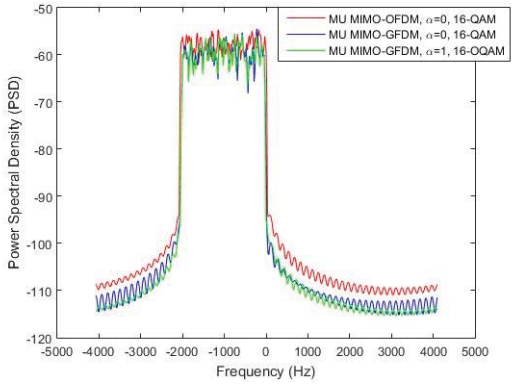

Fig. 7. Comparison OOB Radiation for System Performance

Based on Fig. 7, the attenuation for MU MIMO-GFDM is lower ± 4dB than MU MIMO-OFDM. This indicates OOB radiation of MU MIMO-GFDM is lower than MU MIMO-OFDM due to different pulse shaping usage. MU MIMO-GFDM using RRC pulses with roll of factor (α = 1; 16-OQAM) and (α = 0; 16-QAM), while MU MIMO-OFDM using rectangular pulses with roll of factor (α = 0; 16-QAM). Based on the pulse shaping filter theory in Chapter III, the using of pulse shaping with roll of factor (α = 0) denotes a rectangular pulse, while the roll of factor (0 <α <1) denotes the RRC pulse. The pulse shaping with roll of factor (α) approaches to 1 value, hence it will produce in degradation sidelobe (OOB radiation) in frequency domain, so that the effect of Intercarrier Interference (ICI) can be overcome. Based on these analyzes, the RRC pulse produced a lower sidelobe compared to the rectangular pulse. So that MU MIMO-GFDM system implemented on 5G cellular technology to be able to overcome ICI which can interfere to wireless communication system.

VII. CONCLUSION

In this study, we investigated the performance of Multiuser MIMO-GFDM system using BD linear precoding techniques and MMSE detector to overcome MUI and IAI with lower complexity. MU MIMO-GFDM will be used to overcome the weaknesses of 4G mobile technology which using OFDM waveform. The simulation results show the performance of MU MIMO-GFDM system using RRC pulse shaping and O-QAM moduation is better ±0.84dB than MU MIMO-OFDM and MU MIMO-GFDM using rectangular pulse and QAM modulation. In MU MIMO-GFDM using O-QAM, orthogonality of a waveform can be obtained and low OOB can be reached. PAPR MU MIMO-GFDM is better ±0.578dB than MU MIMO-OFDM, because the number of subcarrier that GFDM used less than OFDM. To analyze the OOB radiation both MU MIMO-OFDM and MU MIMO-GFDM system, we can investigate power spectral density (PSD) curve function of frequency (f). OOB radiation for MU MIMO-GFDM is better ±4dB than MU MIMO-OFDM, because GFDM using RRC pulse and OFDM using rectangular pulse.

Finally, in the next research, we plan to develop performance of MU MIMO-GFDM system with comparing the number of users because MU MIMO is a MIMO application to many users and comparing the antenna scheme because the type of MIMO used is spatial multiplexing.

REFERENCES

[1] T. Kageyama, O. Muta and H. Gacanin, "An adaptive peak cancellation method for linear-precoded MIMO-OFDM signals," 2015 IEEE 26th Annual International Symposium on Personal, Indoor, and Mobile Radio Communications (PIMRC), Hong Kong, 2015, pp. 271-275.

[2] T. Suryani and Suwadi, "Performance Evaluation of MIMO-OFDM Implementation on Wireless Open-Access Research Platform (WARP)", ARPN Journal of Engineering and Applied Sciences, Vol.11, No.23, December 2016.

[3] T. Suryani, Suwadi, Hasan and S. W. Yoga, "Implementation and performance evaluation of orthogonal frequency division multiplexing (OFDM) using WARP," 2015 International Seminar on Intelligent Technology and Its Applications (ISITIA), Surabaya, 2015, pp. 451-456.

[4] Akyildiz IF, Nie S, Lin SC, Chandrasekaran M. 5G roadmap: 10 key enabling technologies. Computer Networks. 2016 Sep 4;106:17-48.

[5] I.S. Gaspar, N. Michailow, "5GNOW: 5G Waveform Candidate Selection", 5GNOW Projects Consortium Group, April 8, 2014.

[6] N. Michailow and G. Fettweis, "Low peak-to-average power ratio for next generation cellular systems with generalized frequency division multiplexing," 2013 International Symposium on Intelligent Signal Processing and Communication Systems, Naha, 2013, pp. 651-655.

[7] A. Farhang, N. Marchetti and L. E. Doyle, "Low complexity GFDM receiver design: A new approach," 2015 IEEE International Conference on Communications (ICC), London, 2015, pp. 4775-4780.

[8] N. Michailow et al., "Generalized Frequency Division Multiplexing for 5th Generation Cellular Networks," in IEEE Transactions on Communications, vol. 62, no. 9, pp. 3045-3061, Sept. 2014.

[9] F. Wang and M.E. Bialkowski, "Performance of Block Diagonalization Scheme for Downlink Multiuser MIMO System with Estimated Channel State Information", Int. J. Communications, Network and System Sciences, Vol. 4, No. 82-87, 2011.

[10] Fang Shu, Wu Gang, and Li Shao-Qian, "Optimal Multiuser MIMO Linear Precoding with LMMSE Receiver", EURASIP Journal on Wireless Communications and Networking Volume 2009, Article ID 197682, 10 pages.

[11] Cho, Yong Soo, Jaekwon Kim, Won Young Yang, and Chung G. Kang. MIMO-OFDM wireless communications with MATLAB. John Wiley & Sons, 2010.

[12] M.H.M. Costa, "Writing on dirty paper", IEEE. Inf. Theory, vol. IT-29, pp. 439-441, May 1983.

[13] H. Weingarten, Y. Steinberg and S. S. Shamai, "The Capacity Region of the Gaussian Multiple-Input Multiple-Output Broadcast Channel," in IEEE Transactions on Information Theory, vol. 52, no. 9, pp. 3936-3964, Sept. 2006.

[14] Q. H. Spencer and M. Haardt, "Capacity and downlink transmission algorithms for a multi-user MIMO channel," Conference Record of the Thirty-Sixth Asilomar Conference on Signals, Systems and Computers, 2002., Pacific Grove, CA, USA, 2002, pp. 1384-1388 vol.2.

[15] Q. H. Spencer, A. L. Swindlehurst and M. Haardt, "Zero-forcing methods for downlink spatial multiplexing in multiuser MIMO channels," in IEEE Transactions on Signal Processing, vol. 52, no. 2, pp. 461-471, Feb. 2004.

[16] S. Shim, J. S. Kwak, R. W. Heath and J. G. Andrews, "Block diagonalization for multi-user MIMO with other-cell interference," in IEEE Transactions on Wireless Communications, vol. 7, no. 7, pp. 2671-2681, July 2008.

[17] I. Gaspar, M. Matthé, N. Michailow, L. Leonel Mendes, D. Zhang and G. Fettweis, "Frequency-Shift Offset-QAM for GFDM," in IEEE Communications Letters, vol. 19, no. 8, pp. 1454-1457, Aug. 2015.

[18] S. W. Yoga, T. Suryani and Suwadi, "Application PTS technique for PAPR reduction in MIMO OFDM using WARP," 2016 International Seminar on Intelligent Technology and Its Applications (ISITIA), Lombok, 2016, pp. 317-322.

[19] Gaspar I.S., "Waveform Advancements and Synchronization Techniques for Generalized Frequency Division Multiplexing ", PhD diss., Dresden, Technische Universitat Dresden, Diss.